

Plasma dynamics in a multimirror magnetic system

V. V. Danilov and É. P. Kruglyakov

Institute of Nuclear Physics, Siberian Branch, USSR Academy of Sciences

(Submitted December 8, 1974)

Zh. Eksp. Teor. Fiz. **68**, 2109–2115 (June 1975)

An experimental study is reported of the behavior of plasma in a multimirror trap for fast ($\tau \ll L/v_{Ti}$) beam switching. It is shown that, in the case of small-scale corrugations ($l < \lambda < L$), the behavior of the plasma is in quantitative agreement with the theory of plasma confinement in a multimirror magnetic field.

PACS numbers: 52.55.H

1. INTRODUCTION

The experiments reported in,^[1-3] which were designed to verify the longitudinal confinement of dense plasma in a multimirror magnetic trap as proposed by Budker et al.,^[4] show that the theoretical description of longitudinal transport processes is substantially in agreement with experimental results. For the most interesting case, where the mean free path of the ions, λ_i , was less than the total length L of the system, but greater than the length l of an individual mirror trap, the theory^[4-6] shows that the behavior of plasma in the multi-mirror trap is described by

$$\frac{\partial n}{\partial t} = \xi \frac{\partial}{\partial z} \frac{1}{n} \frac{\partial n}{\partial z}, \quad (1)$$

where ξ/n has the significance of the longitudinal diffusion coefficient of the plasma.^{[5] 1)}

Previous experiments^[1-3] were largely concerned with the case where $\partial n/\partial t = 0$ and (1) could be used to determine the axial density distribution for time-independent plasma flows along the magnetic field with a particular form of the longitudinal diffusion coefficient:

$$n(z) = n_L \exp\left(A \frac{L-z}{\lambda_L}\right) \approx n_L \exp\left(\frac{L-z}{\lambda_L}\right). \quad (2)$$

In this expression n_L and λ_L are respectively the plasma density and ion mean free path at exit from the system at the point where the density is measured. The coordinate z is measured from the opposite end of the system. The experiments reported in^[1-3] confirm the validity of (2). Logan et al.^[7] have independently observed an increase in the density along the axis of the multi-mirror trap under time-independent conditions.

For time-dependent conditions ($\partial n/\partial t \neq 0$), the theory predicts a substantial increase in the plasma confinement time as compared with the free-diffusion time in a uniform magnetic field. Experiments with fast beam switching^[2,3] have, in fact, shown an increase in the plasma decay time, but quantitative comparisons with this theory were not made. The aim of the present research was to carry out a quantitative comparison between the results of time-dependent experiments (fast switching of the plasma beam) and theory.

2. APPARATUS

The cesium plasma apparatus was described previously in^[1,2]. The magnetic system consisted of 14 mirror traps, each 16 cm long, and could be used to produce a mirror field of $H_{\max} = 5400$ Oe with a mirror ratio $K = 1.83$. The cesium was surface-ionized on a hot tantalum plate ($T_0 = 2100-2450^\circ\text{K}$).^[2] Because of its large Coulomb cross section, the low-temperature alkali-metal plasma could be used to simulate longitudi-

nal transport in dense plasma, subject to the theoretical condition $l < \lambda_i < L$.

The plasma density was measured with thin baked Langmuir probes, usually located on the axis of the system at geometrically equivalent points in the successive traps at which the magnetic field was $H = 0.72H_{\max}$. Provision was made for the radial displacement of the probes to facilitate determinations of the transverse diffusion coefficient from the magnitude of $\partial n/\partial r$ (see^[8,9]). (The experiments show that the transverse diffusion coefficient is much greater than the Bohm value, which means that transverse losses are unimportant in the experiments described below).

The pulsed ($\sim 0.25 \mu\text{sec}$ duration) switching (on and off) of the neutral-cesium beam was carried out mechanically with the aid of a shutter in the form of a carefully ground, slotted cup driven by a strong spring in a cylindrical container filled with cesium vapor.

3. STEADY FLOW OF PLASMA

Before we discuss time-dependent effects, we must consider an example of the time-independent distribution of density along the axis of the system, and note one particular feature.

Figure 1a shows an oscillogram illustrating the inhomogeneous character of the time-independent distribution of plasma density along the axis. The oscillogram was obtained as follows. Probes of equal sensitivity in

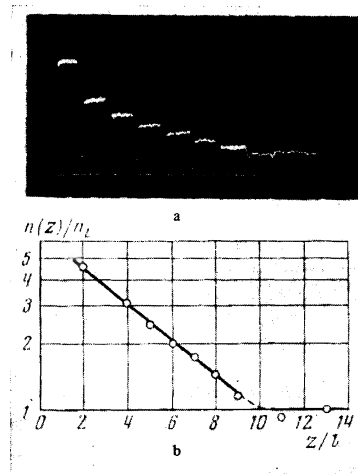


FIG. 1. Steady-state distribution of plasma density along the axis of the multimirror system: a—probe signals recorded by successive probes in the different traps; b—longitudinal distribution of plasma density in the multimirror magnetic field, $n_L = 10^{10} \text{ cm}^{-3}$, $\lambda_L = 85 \text{ cm}$.

traps 2, 4–9, 11, and 23 were, in turn, connected to the oscillograph input (the traps are numbered from the ionizer which is located in trap No. 1). It is clear from the oscillogram that the plasma density does, in fact, increase in the direction of the ionizer. Figure 1b shows the reduced density³⁾ $n(z)/n_L$ on the axis for this oscillogram. There is good agreement between experiment and theory [Eq. (2)].

The diffusive flow illustrated in the above graph is described by (2) over a length equivalent to, say, ten mirror traps. The character of the flow undergoes a change over a distance of $\sim 4l$ from the exit. This effect has a simple explanation. Near the exit from the system, at distances less than the mean free path, there are no collisions between the transmitted and trapped particles and, therefore, there is no density gradient. Therefore, the quantity L in (2) must be interpreted not as the length of the system, but the effective length L_{eff} over which the diffusive flow takes place.

4. ESTABLISHMENT OF TIME-INDEPENDENT DISTRIBUTION

When $l < \lambda_i < L$, the character of the flow resembles the diffusive transport of plasma from trap to trap. One would therefore expect that the time-independent density distribution would be established in the system in a time $t \gg L/v_{Ti}$. This was confirmed qualitatively in^[10]. In the present work, the experimental results on the attainment of time-independent flow were compared with numerical solutions of (1) produced by a computer.

Figure 2 shows oscillograms demonstrating the behavior of plasma density as a function of time at two points in the system (n_{11} and $n_1 \approx n_L$) after the beam was rapidly switched on.⁴⁾ We note an interesting feature of the oscillogram, which refers to the measured density $n_{11}(t)$. The increase in density does not begin immediately after the leading front of the plasma current has passed through the probe, but only after a certain time interval. This is clear from Fig. 2c (see also Fig. 2 in^[10]). The appearance of the plateau on the

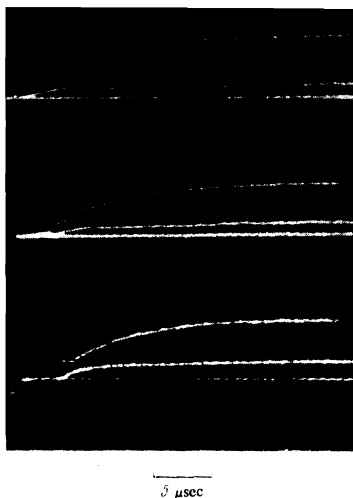


FIG. 2. Plasma density $n_{11}(t)$ —upper trace and $n_1(t)$ —lower trace when the beam is rapidly switched on: a) $n_L(\infty) = 1.2 \times 10^{10} \text{ cm}^{-3}$, $n_{11}/n_L = 5.0$, $T_i = 0.55 \text{ eV}$; b) $n_L(\infty) = 1.2 \times 10^{10} \text{ cm}^{-3}$, $n_{11}/n_L = 4.3$, $T_i = 0.67 \text{ eV}$; c) $n_L(\infty) = 6.1 \times 10^9 \text{ cm}^{-3}$, $n_{11}/n_L = 3.3$, $T_i = 0.48 \text{ eV}$.

oscillograms has a simple explanation: effects associated with “friction” between transmitted and trapped particles can appear only after the plasma front has departed from the ionizer to a distance exceeding the ion mean free path, because collisions transforming transmitted particles into trapped particles begin to have an effect after a time $\tau \sim \lambda_i/v_{Ti}$. As the plasma density in the beam increases, i.e., λ decreases, the plateau length is found to decrease. This was, in fact, observed in our experiments (Figs. 2a and 2b).

Probe signals representing the concentration $n_i(t)$ have a different appearance.⁵⁾ In this case, the rapid increase in density ceases after a time $\sim L/v_{Ti}$. The subsequent slow increase in the density n_i is explained by the “nonconservation” of the current while the time-independent state is being established in the system, because some of the current is expended in the formation of the gas of trapped particles. Once time-independent flow has been established (end of sweep), the plasma density n_i becomes equal to the plasma density n_{11} on the plateau, and this indicates the absence of transverse losses in the system.

Experimental data on the establishment of time-independent flow are thus in relatively good agreement with the theoretical predictions in^[4–6]. For quantitative purposes, the experimental results were compared with numerical computer solutions of (1), subject to the following boundary and initial conditions:

$$\begin{aligned} -\frac{H_0}{H_{\text{max}}} \xi \frac{1}{n} \frac{\partial n}{\partial z} &= q_0, \quad z=0; \\ -\frac{H_L}{H_{\text{max}}} \xi \frac{1}{n} \frac{\partial n}{\partial z} &= q_L, \quad z=L_{\text{eff}}; \\ n(z) &= 0, \quad t \leq 0, \end{aligned} \quad (3)$$

where q_L is the current density at exit from the system^[2] at the point where the density is measured by the last probe

$$q_L = \frac{H_L}{H_{\text{max}}} \frac{n_L v_{Ti}}{\sqrt{\pi} [1 - (1 - H_L/H_{\text{max}})^{1/2}]} = 0.86 n_L v_{Ti} = n_L \bar{v}, \quad (4)$$

and q_0 is the density of the current from the ionizer ($q_0 \approx q_L$). Since the ionizer is located in magnetic field H_0 which is not very different from H_L , it was assumed in the calculations that $q_0 = q_L$. The ratio L_{eff}/λ_L , determined experimentally, was used as the parameter in the calculations.

Equation (1) is valid in the region where diffusive flow takes place. It is clear from Fig. 1 that the total length of the system can serve as the length parameter L_{eff} only approximately. Precise determination of the effective length L_{eff} was carried out as follows. Establishment of the time-independent plasma flow during pulsed beam switching was investigated simultaneously with seven probes placed in traps 11, 9, 7, 5, 3, and 1 (counting from the last probe). Simultaneous detection of signals by all seven probes (only two signals are shown in Fig. 2) enables us to obtain the time-independent density distribution along the axis of the system in each individual experiment. By plotting this dependence in the form $\ln[n(z)/n_L] = f(z)$, we can immediately determine two parameters, namely, the effective length within which the diffusive flow of the plasma takes place (L_{eff}) and the ratio L_{eff}/λ_L .

Let us now consider the accuracy of the comparison between the experimental results and the numerical solution of (1). The argument of the exponential in (2) is known to within the factor A which cannot be calcu-

lated analytically. However, it is known that $A \sim 1$ (see^[2]). The ion mean free path λ_L can therefore be determined from the experimental data using (2) to within the undetermined factor $A \sim 1$. On the other hand, the mean free path λ_L is related to the ion temperature T_i by the formula

$$\lambda_L \approx 3 \cdot 10^{12} T_i^2 [\text{eV}] / n_L.$$

Hence it is clear that T_i is determined to within \sqrt{A} and, since the computer calculations were carried out with $\tau = H_L L_{\text{eff}} / H_{\text{max}} \tilde{v} \propto v_{T_i}^{-1}$ as the unit of time, the main error in the comparison between experimental and theoretical results was connected with the accuracy with which the thermal velocity of the ions, i.e., $A^{1/4}$, was found.

Figure 3 shows results of the comparison between experimental results (solid lines) and theoretical calculations (the experimental curves correspond to the oscillograms in Fig. 2). Remembering our remark about the accuracy with which the thermal velocity v_{T_i} of the ions can be determined, i.e., the accuracy with which the time scales can be made to coincide, we may conclude that the agreement between theory and experiment is very good in the case of Figs. 3b and 3c. The substantial discrepancy in Fig. 3a for $n_{11}/n_L \approx 4$ can be explained as follows. Equation (1) with diffusion coefficient $D \propto n^{-1}$ is valid for $\lambda > L$. For $\lambda < L$, the behavior of the plasma is described by another equation with a diffusion coefficient $D \propto n$ (see^[6]). In the case of Fig. 3a, $\lambda_L = 77$ cm in time-independent flow, so that the mean free path λ_{11} in the region of the probe providing the signal in Fig. 2a is formally equal to the length l of the trap when $n_{11}/n_L = 4.8$. In view of the remarks made above with regard to the accuracy with which the ion mean free path can be determined ($\sim A$), this explanation of the observed discrepancy between experiment and theory may be regarded as entirely reasonable.

5. DYNAMICS OF PLASMA DECAY

We must now consider the comparison between theory and experiment in the case of fast switching off of the beam. Under the conditions of these experiments ($l < \lambda < L$), the behavior of the plasma density $n(z, t)$ should, as before, be determined by (1). The following expressions were used as the boundary and initial conditions:

$$\left. \begin{aligned} \partial n / \partial z = 0, & \quad z = 0 \\ -\frac{H_L}{H_{\text{max}}} \xi \frac{1}{n} \frac{\partial n}{\partial z} = q, & \quad z = L \end{aligned} \right\} t > 0,$$

$$\frac{n(z)}{n_L} = \exp \left[\frac{q_L L H_{\text{max}}}{\xi H_L} \left(1 - \frac{z}{L} \right) \right] = \exp \left[\frac{L}{\lambda_L} \left(1 - \frac{z}{L} \right) \right], \quad t \leq 0. \quad (5)$$

The first boundary condition corresponds to the absence of the current from the ionizer after the beam has been switched off (it is assumed that plasma recombination on the ionizer is unimportant).

As in the last section, the ratio L_{eff}/λ_L is used as the parameter in the calculations. The results of the calculations were compared with experimental data on plasma decay half-life in^[2] (see Fig. 6a in^[2]).⁶

Before we proceed to a comparison of the results, we must make the following points.

1. The effective size of the region of diffusive plasma flow was not determined in^[2]. The distribution in space of the plasma density was, however, subse-

quently investigated in a broad range of parameters in^[10]. These data were then used to deduce the values of L_{eff} for the values of n_0/n_L reported in^[2]. This procedure did, of course, reduce somewhat the accuracy of the comparison.

2. The remark made in the last section about the uncertainty in the comparison of time scales, due to the uncertainty in the numerical coefficient A , is also valid in the present case.

Figure 4 shows the experimental plasma half-life $\tau_9^{1/2}$ as a function of the exit density n_L . The solid curve was obtained by numerical solution of (1). Since both the change in density over the length of the system and the effective length L_{eff} decrease with decreasing n_L , and the uncertainty in L_{eff} increases, we have confined the comparison to the region of the maximum effect, where the errors are at a minimum. As can be seen from Fig. 4, the agreement between experiment and theory is completely satisfactory.

Figure 5 shows the plasma density $n_0(t)$ as a function of time after the beam was switched off. The solid curve corresponds to the oscillogram given in Figs. 5a in^[2]. As can be seen, the agreement between theory and experiment is satisfactory. The departure of the calculated curve from the experimental results is observed after about msec, when $n_0(t) < 3 \times 10^9 \text{ cm}^{-3}$ [$n_0(0) = 1.3 \times 10^{10} \text{ cm}^{-3}$] and $\lambda_0 \sim L$. Equation (1) is not valid in this region.

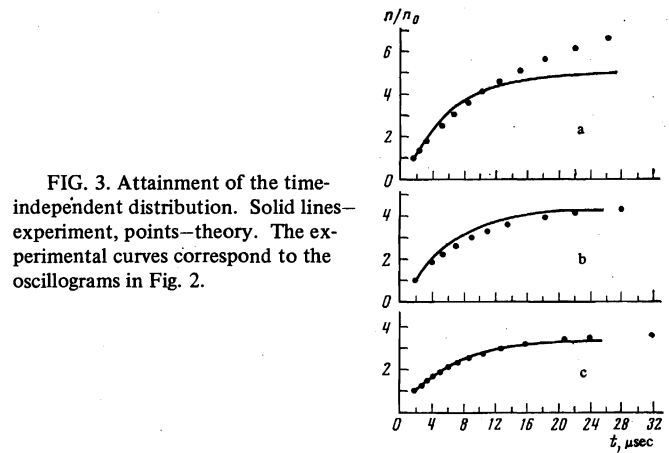


FIG. 3. Attainment of the time-independent distribution. Solid lines—experiment, points—theory. The experimental curves correspond to the oscillograms in Fig. 2.

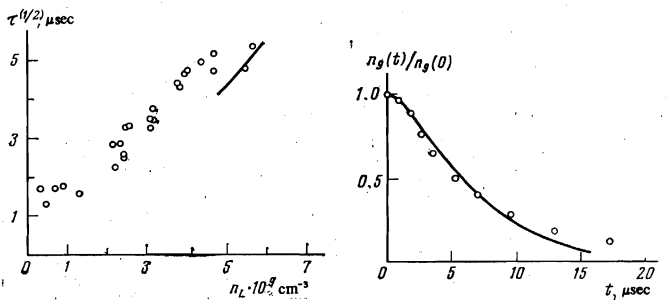


FIG. 4

FIG. 5

FIG. 4. Plasma half-life $\tau_9^{1/2}$ as a function of the plasma density at exit from the trap: points—experimental, curve—theoretical.

FIG. 5. The function $n_0(t)$ after the beam has been cut off; $n_0(0) = 5.4 \times 10^9 \text{ cm}^{-3}$. Points—experimental, solid curve—theoretical.

We may therefore conclude that the totality of the experimental data shows that, for parameter values which are of the greatest interest for thermonuclear applications ($l < \lambda < L$), Eq. (1) provides a correct description of longitudinal transport processes. It can therefore be used with confidence in problems connected with the confinement of dense thermonuclear plasma in multimirror magnetic traps.

The authors are indebted to V. V. Mirnov and D. D. Ryutov for useful discussions and to P. Z. Chebotaev for assistance in the numerical calculations.

¹We note that the transport of matter is determined by (1), subject to the condition that the plasma temperature is uniformly distributed along the length of the system ($\partial T/\partial z = 0$) and is time-independent. These conditions were satisfied in the majority of our experiments.

²In [¹⁻³], the ionization was produced by a hot tungsten surface ($T_0 = 2400^\circ\text{K}$).

³The density n_L was measured in the next-to-last trap.

⁴Here and henceforth, the numerical subscript of n represents the position of the probe. In particular, n_{11} means that the concentration was measured by the probe at a distance of 11 traps from the last probe.

⁵We note that $n_1 \approx n_L$ and $n_L \propto q_L$ [see Eq. (4)]. The quantity n_1 can therefore also serve as a measure of the current.

⁶In [²], the decay of the plasma was investigated at a point separated from the last probe by a length equivalent to nine traps.

¹G. I. Budker, V. V. Danilov, É. P. Kruglyakov, D. D. Ryutov, and E. V. Shun'ko, ZhETF Pis'ma Red. 17, 117 (1973) [JETP Lett. 17, 81 (1973)].

²G. I. Budker, V. V. Danilov, É. P. Kruglyakov, D. D.

Ryutov, and E. V. Shun'ko, Zh. Eksp. Teor. Fiz. 65, 562 (1973) [Sov. Phys.-JETP 38, 276 (1974)].

³V. V. Danilov, É. P. Kruglyakov, and E. V. Shun'ko, Proceedings of the Sixth European Conference on the Physics of Plasma and the Problem of Controlled Thermonuclear Fusion, JINR, 1973, p. 415.

⁴G. I. Budker, V. V. Mirnov, and D. D. Ryutov, ZhETF Pis'ma Red. 14, 320 (1971) [JETP Lett. 14, 212 (1971)].

⁵G. I. Budker, V. V. Mirnov, and D. D. Ryutov, Trudy Mezhdunar. konf. po teorii plazmy (Proceedings of International Conf. on the Theory of Plasma), Naukova Dumka, Kiev, 1971, p. 145.

⁶V. V. Mirnov and D. D. Ryutov, Nuclear Fusion 12, 627 (1972).

⁷B. G. Logan, J. G. Brown, M. A. Lieberman, and A. J. Lichtenberg, Phys. Rev. Lett. 29, 1435 (1972).

⁸A. A. Ivanov, Ya. R. Rakhimbabaev, and V. D. Rusanov, Zh. Eksp. Teor. Fiz. 52, 833 (1967) [Sov. Phys.-JETP 25, 545 (1967)].

⁹N. S. Buchel'nikova, R. A. Salimov, and Yu. I. Éidel'man, Zh. Eksp. Teor. Fiz. 52, 837 (1967) [Sov. Phys.-JETP 25, 548 (1967)].

¹⁰G. I. Budker, V. V. Danilov, V. A. Kornilov, É. P. Kruglyakov, V. N. Luk'yanov, V. V. Mirnov, and D. D. Ryutov, Proc. Fifth Intern. Conf. on Plasma Physics and Controlled Fusion Research, NIAEA-CN-33/118-3, Tokyo, 1974.

Translated by S. Chomet

225